Energy 312 (2024) 133588

Contents lists available at ScienceDirect

Energy

journal homepage: www.elsevier.com/locate/energy

HeatNetSim: An open-source simulation tool for heating and cooling networks suitable for future energy systems

Sina Dibos [a,b,*], Thiemo Pesch [a], Andrea Benigni [a,b,c]

[a] Forschungszentrum Jülich GmbH, Institute of Climate and Energy Systems, ICE-1: Energy Systems Engineering, Jülich, 52425, Germany
[b] RWTH Aachen University, Aachen, 52062, Germany
[c] JARA-Energy, Jülich, 52425, Germany

ARTICLE INFO

Keywords:
Bidirectional network
District heating and cooling
Energy system simulation
Simulation tool
Waste heat integration

ABSTRACT

Low temperature district heating and cooling networks are a promising solution to increase the share of renewable energy within the heating and cooling sector. However, the transition to bidirectional networks poses new challenges (representation of fluid-specific properties, coordinate operation with power grid, retrofitting of existing networks) requiring a new generation of simulation tools. In this paper, we present a simulation tool for thermal networks capable of bidirectional flows, zero mass flows and a dynamic temperature calculation. The structure of the tool allows coupling to other sector's simulation tools enabling multi-domain analysis of relevant interactions with power and gas grids. We showcase the tool with two case studies inspired by the heating and cooling infrastructure of our campus. The first case study analyzes the operation of a unidirectional high temperature district heating network supplied by a power-driven combined heat and power plant. The case study highlights the suitability of district heating networks as a source of flexibility to the power grid by using its thermal inertia. The second case study investigates the transition from independently operated district heating and district cooling networks into a bidirectional low temperature district heating and cooling network highlighting the energy saving potential by thermal balancing effects.

1. Introduction

Climate change requires decarbonization strategies for the energy sectors power, gas and heat. Within the last decades, the efforts mainly focused on the electricity sector with increasing expansion of renewable power production by wind and PV systems [1]. However, the generation of heat for space heating and domestic hot water has great share within the total greenhouse gas emissions [2]. Within the EU, the heating and cooling sector accounts for 50% of the total energy consumption of end users [1], while the heat generation is mainly based on fossil fuels (to 60%) [2]. As renewable energies only generate about one quarter of the total domestic heat demand [3], one opportunity is seen in an increased use of district heating (DH) networks. These can integrate a variety of renewable and commercial waste heat sources and thus drive forward the decarbonization targets within the heating sector [4,5]. However, the degree of enhancement strongly depends on the situation within the investigated country, such as electricity mix and existence of combined heat and power (CHP) plants [6]. In terms of sector coupling, DH networks with their inherent thermal inertia can provide flexibility to the electricity sector, e.g. through the electricity-driven use of heat pumps (HPs) [7] and CHP plants within thermal boundaries [8]. This can play a particularly important role in local energy communities that have limited systemic flexibility.

Lund et al. [9] define four generations of DH networks varying in their time of application and functionalities. Between the first and the fourth generation, the temperature level of the network decreases and the energy efficiency increases. The first generation is characterized by steam as a heat transfer medium and is operated on temperatures up to 200 °C, while the second generation uses pressurized water with temperatures more than 100 °C. First and second generation DH networks are exclusively supplied by fossil fuels, while the third generation integrates alternative energy sources, such as biomass and industrial waste heat. With the fourth generation (40 °C to 70 °C) more renewable energy sources, mainly geothermal and solar energy, are integrated into the system. A further development of thermal networks is seen in the usage of low temperature district heating and cooling (LTDHC) networks. The European Commission [10] refers to these networks as fifth generation networks, while Lund et al. propose in [11] that these networks are a parallel development of the fourth generation. LTDHC networks are characterized by bidirectional flows and their

* Corresponding author at: Forschungszentrum Jülich GmbH, Institute of Climate and Energy Systems, ICE-1: Energy Systems Engineering, Jülich, 52425, Germany.
E-mail address: s.dibos@fz-juelich.de (S. Dibos).

https://doi.org/10.1016/j.energy.2024.133588
Received 19 December 2023; Received in revised form 27 July 2024; Accepted 22 October 2024
Available online 30 October 2024

Nomenclature

Abbreviations

CHP	Combined Heat and Power
COP	Coefficient of Performance
DC	District Cooling
DH	District Heating
DHC	District Heating and Cooling
EBU	Energy Balancing Unit
EER	Energy Efficiency Ratio
FZJ	Forschungszentrum Jülich
HP	Heat Pump
HPC	High Performance Computer
LTDHC	Low Temperature District Heating and Cooling
NR	Newton Raphson

Symbols

α	Heat transfer coefficient
$\dot{m}$	Mass flow rate
$\dot{Q}$	Heat flow
$\dot{V}$	Volume flow rate
η	Efficiency
λ	Heat conductivity
μ	Viscosity
$\overline{v}$	Mean fluid velocity
ρ	Density
A	Area of pipeline
C	Heat capacity
c_p	Specific heat capacity
D	Diameter of pipeline
f	Friction factor
k_s	Roughness of material
l	Length
P	Electricity
r	Radius of pipeline
Re	Reynolds number
T	Temperature
t	Time
V	Volume
v	Fluid velocity

Subscripts

amb	Ambient
CD	Cooling Demand
el	Electricity
HD	Heating Demand
HE	Heat Exchanger
in	Inflow
out	Outflow

temperature level nearby ambient temperature (6 °C to 40 °C) [11]. The low operating temperature yields reduced heat losses within the distribution system [12] and the integration of different kinds of waste heat sources [13]. Furthermore, LTDHC networks enable a simultaneous supply of heating and cooling energy leading to cost reductions regarding electricity consumption and operational efforts [14]. This is relevant in terms of an increasing cooling demand, while exclusive district cooling (DC) networks still play a minor role in European countries [15]. LTDHC networks can therefore expand the decarbonization strategies on the cooling sector, which is essential for future developments of DC systems [16].

1.1. Modeling approaches

Several approaches exist in literature to calculate and simulate the hydraulic and thermal properties of DH and district heating and cooling (DHC) networks. As the temperature variation within a thermal network is slower compared to the pressure distribution, the hydraulic and thermal properties can be calculated in a coupled or decoupled approach. The decoupled approach solves the hydraulic problem first – commonly with the Hardy-Cross [17] or Newton–Raphson algorithm [18] – and the resulting values of the mass flow rates can be used in the following thermal calculation. The coupled approach calculates the hydraulic and thermal problem in one matrix [18], which is then usually solved by the Newton–Raphson algorithm [19] or the Jacobi method [20]. The coupled approach leads to fewer iterations within the solution process and therefore to a faster convergence compared to the decoupled approach [18,19]. However, the larger Jacobian matrix within the coupled approach results in a higher computation time.

Based on the coupled and decoupled approach, three major modeling approaches exist. These approaches vary in their calculation of the temporal temperature distribution, while the hydraulic properties are commonly assumed to be steady-state, except of some works like [21]. The steady-state approach neglects hydraulic and thermal dynamics, while the dynamic approach includes the thermal transmission delay within the pipelines and nodes over time [19]. The quasi-dynamic approach is a simplification of the dynamic approach, only considering the temporal temperature distribution within each node [22].

For steady-state simulations, both the coupled and decoupled approach can be applied. Especially analyzes of multi energy systems use steady-state approaches, as their computational power is to be minimized [23,24] and a detailed thermal distribution within DH or DHC networks might not be of main interest. Analogue to the steady-state approach, quasi-dynamic approaches can be based on coupled or decoupled calculations, while in literature only the decoupled approach exists [23]. However, Dancker and Wolter [19,25] introduce a quasi-steady-state coupled calculation approach. Within quasi-dynamic simulations, the flow is represented either by an Eulerian or a Lagrangian method. Within the Eulerian method, specific locations within the network are observed, while water segments flow through these locations [23]. In contrast, the Lagrangian method focuses on the water segments themselves [19], also referred to as the plug-flow method [26,27]. The quasi-dynamic approach is commonly based on the *node method*, where the transmission delays of the thermal properties are exclusively stored in the nodes and the temperature or thermal distribution between the nodes stays unknown [22]. One advantage of the *node method* are the small computational times, as only the incoming water segment propagation time is calculated together with the thermal losses. This goes along with the slightly reduced accuracy due to the mixing of water segments temperatures in one single node [28]. If temperature data between the nodes needs to be known, a thermal dynamic approach can be applied. The dynamic approach can be based on several methods, such as the *element method* [29] or the *node method* [30]. Some works extend these methods to the *finite difference method* [31–33], the *function method* or the *method of characteristics* [27]. Although achieving more accurate thermal results by the usage of a dynamic calculation, computational times are significantly higher compared to steady-state or quasi-dynamic approaches [26]. The specific use case should therefore set the priority between a more accurate simulation or reduced computational costs.

Table 1
Overview of published open-source tools and libraries for the simulation of thermal networks.

Tool/Library	License	Bidirectional flows	Thermal-hydraulic modeling approach	Modeling Language	Remarks
DHNx	open-source	✗	steady-state	Python	
DiGriPy	open-source	✗	steady-state	Python	
pandapipes	open-source	✗	steady-state	Python	Focus on MES simulations
nPro	Required for commercial users	✓	dynamic	Python	Not extendable by user
AixLib	Requires Dymola/OpenModelica	✓	dynamic	Modelica	
TransiEnt	Requires Dymola	✗	quasi-dynamic	Modelica	
IDEAS	Requires Dymola/OpenModelica	✓	dynamic	Modelica	
This tool	open-source	✓	quasi-dynamic	Python	

1.2. Existing tools

There are several tools available for modeling and simulating thermal networks based on the approaches presented in the previous section. Commercial tools like STANET [34], TRNSYS [35] or ROKA^3 [36] usually provide a well-prepared user interface and a good costumer support. However, this paper concentrates on open-source tools, as these provide a high level of transparency and reproducibility, which can have a positive impact on the development of research activities [37].

Published open-source tools for modeling and simulation of thermal networks are DHNx [38], DiGriPy [39], pandapipes [40], nPro [41] and some open-source modeling libraries such as TransiEnt [42], AixLib [43] or IDEAS [44] (see Table 1).

The tool DHNx is written in Python and the used components are based on the open-source Open Energy Modeling Framework (oemof) [38]. It can be used for optimization, as well as hydraulic and thermal simulation of DH networks [45]. Nevertheless the tool does not consider dynamics within the flow and heat transfer. DiGriPy has the same area of application as DHNx [39], while also focusing on the steady-state approach. Another open-source tool is pandapipes [40], which is a complementary development of the power grid simulation tool pandapower [46]. Pandapipes is a steady-state tool for the simulation of gas and heating networks and has a strong focus on coupled simulations of the sectors power, gas and heat [40]. The three mentioned tools have their emphasis on the simulation of unidirectional networks and do not provide the possibility of simulating bidirectional flows. This feature is available within the tool nPro [41], which is a software tool for planning district energy systems such as DH and DHC networks. However, nPro lacks of the possibility of individual extensions by the user and cannot be coupled with other energy sectors.

There are several Modelica-libraries enabling dynamic simulations. TransiEnt is developed for the simulation of multi energy grids with a focus on the integration of renewable energies. The library uses basic components such as pipeline models from the Modelica-library ClaRa [47] and extends these [48]. However, TransiEnt is not capable of modeling bidirectional networks. Moreover, the commercial Modelica environment Dymola is used to perform the simulation [49]. The library AixLib [43] has a focus on modeling and analyzing buildings and distribution networks in the context of urban energy systems [50] and is capable of modeling and simulating bidirectional networks.

1.3. Goal of this paper, contribution and paper structure

The presented review demonstrates that there are several open-source tools for the simulation of DH networks, however, the mentioned Python based tools use a steady-state approach and are not capable of bidirectional flows. This feature is possible within some of the presented Modelica-libraries. However, the commercial software Dymola is still mostly applied for research purposes instead of the free version OpenModelica. Moreover, Modelica faces several issues regarding the simulation of large-scale DH or DHC networks [51].

Consequently, there exists no further development of a DH simulation tool enabling the following characteristics and functionalities:

- non-proprietary software, extendable
- capable of bidirectional flows and zero mass flow
- capture thermal transmission delay (quasi-dynamic)
- suitable for the integration into a MES simulation framework

The first major contribution of this paper is to close the recognized gab by providing a thermal-hydraulic simulation tool enabling the mentioned advanced concepts and properties. Secondly, the two presented case studies show that DH networks coupled to power-driven CHP plants can provide flexibility to the power grid by adapting the supply temperature. Moreover, we demonstrate that bidirectional LTDHC networks can achieve a high energy saving potential by thermal balancing effects.

The paper is structured as follows: The development of the simulation tool is presented in Section 2, starting with the explanation of the component models in Section 2.1. This is followed by the description of the simulation flow in Section 2.2, where we describe the generation of the network structure and explain the applied solution algorithm. We verify the pipeline model with a state-of-the art plug flow pipe model in Section 3 and show results for the flow and heat transfer. The simulation tool is firstly applied within two case studies in Section 4 showing the tool's capability to be coupled to other energy sectors and control algorithms and stressing the energy saving potentials of bidirectional networks. We conclude our paper with by summarizing the main findings in Section 5.

2. HeatNetSim

HeatNetSim is an open-source tool, written in Python, which is designed for the thermal-hydraulic simulation and operational control of thermal networks. The tool's modular structure based on Python classes enables an easy extensibility, modification and substitution of single elements, such as component models or solvers.

The tool enables a quasi-dynamic approach with a steady-state hydraulic calculation and a dynamic temperature calculation. The consideration of thermal dynamics is implemented to increase the scope of application, as thermal dynamics are especially relevant for network operation changes [52]. However, in case the user prefers faster computing times instead of a more detailed thermal representation, a purely steady-state approach can be chosen. The hydraulic and thermal properties are calculated by using the decoupled approach, according to Section 1.1. We apply the *node method*, while the temperature calculation is based on the Eulerian method. This enables us to limit computational power, which is especially relevant when coupling the tool to other domains.

For the modeling of the components, we meet the following assumptions:

- the water is considered as an incompressible and homogeneous fluid
- the flow is considered as one-dimensional and fully developed
- the material has constant properties
- gravity effects are neglected
- the time step is constant

2.1. Modeling

DH and DHC networks consist of the prosumers exchanging heat with the thermal network, while the substation serves as an interface between the building and the thermal network. The network consists of a pipeline system connecting the prosumers with the energy balancing unit (EBU) supplying the residual heating or cooling energy.

2.1.1. Pipeline model

The pipeline model guarantees the correct calculation of pressure and heat losses, divided into a hydraulic and a thermal calculation part. Within the hydraulic calculation of HeatNetSim, we distinguish between laminar and turbulent flows, characterized by the Reynolds number of the flow. Based on that, the pressure difference between inlet and outlet node and the occurring mass flow rate is determined (for a detailed mathematical description, see Appendix A). The resulting mass flow rate is then applied within the non-linear heat loss calculation taking the heat transfer coefficient and the ambient temperature into account Appendix B.

The pipeline wall serves as an inertia in the network system, which can be modeled as a volume within each pipeline segment. The size of the volume V_{wall} is calculated from Eq. (1) with C_{wall} being the heat capacity of the pipe wall.

$$V_{wall} = \frac{C_{wall}}{\rho c_p} \tag{1}$$

The final outlet temperature $T(l)'$ of the pipeline is calculated in Eq. (2). Hereby, $\dot{V}$ is the volume flow rate, Δt_{step} the time step length of each simulation and $T_{wall}(t_{i-1})$ is the wall temperature of the previous time step.

$$T(l)' = \frac{\dot{V}\Delta t_{step} T(l) + V_{wall} T_{wall}(t_{i-1})}{\dot{V}\Delta t_{step} + V_{wall}} \tag{2}$$

According to the described *node method* in Section 1.1, the thermal transmission delay is considered between two neighboring nodes. Therefore, we assume a constant flow velocity within an individual pipeline for an individual time step. The fluid travels in flow batches through the pipeline system and we calculate the time when the frontier of an incoming batch reaches a specific node. Therefore, $t_{in}(i)$ represents the arrival time for node i, $t_{in}(i+1)$ the arrival time for the neighboring node i+1 and $v_{flow}(i)$ the velocity of the flow in pipeline i:

$$t_{in}(i+1) = t_{in}(i) + \frac{l}{v_{flow}(i)} \tag{3}$$

The flow velocity of pipeline i is calculated equation in (4):

$$v_{flow}(i) = \frac{\dot{m}_{flow}(i)}{\rho A} \tag{4}$$

2.1.2. Substation

For the heat transfer within the substation, we model a heat exchanger, a HP and a compression chiller. According to the applied control algorithm *variable Flow Constant Temperature (VF-CT)*, a decentral circulation pump is used to provide the mass flow rate within the network.

The heat exchanger can be used for heating and cooling purposes and is explained in Appendix C. The HP model is based on an energy balance and a variable coefficient of performance (COP) calculation according to the network and demand temperature Appendix D, while the compression chiller is modeled analogue, but with a constant efficiency Appendix E.

After calculating the thermal demand on the primary side of the network, Eq. (5) determines the corresponding mass flow rate $\dot{m}_{flow}$. $T_{network,in}$ and $T_{network,out}$ represent the temperature values of the inlet and outlet node of the substation.

$$\dot{m}_{flow} = \frac{\dot{Q}_{network}}{c_p(T_{network,in} - T_{network,out})} \tag{5}$$

The electricity consumption of the circulation pump can be calculated according to the following equation [53]:

$$P_{el} = \frac{\dot{m}_{flow}\Delta p}{\rho \eta_h \eta_m}. \tag{6}$$

Hereby, Δp is the pressure difference between the inlet and outlet node of the circulation pump, η_h is the hydraulic efficiency and η_m the motor efficiency.

2.1.3. Waste heat source

The waste heat source is modeled analogue to the heat exchanger, together with the mass flow calculation from of Eq. (5). To guarantee a physically possible heat exchange, a controller checks if the waste heat temperature is high enough to be cooled by direct cooling from the network.

2.1.4. Energy balancing unit

The EBU balances the difference between the overall heating and cooling demand by rising or lowering the temperature of the incoming flow. The temperature of the outgoing flow is set to the predefined temperature T_{warm} in case of a positive mass flow and to T_{cold} in case of a negative mass flow:

$$T_{out} = \begin{cases} T_{warm}, & \dot{m}_{flow} > 0 \\ T_{cold}, & \dot{m}_{flow} < 0. \end{cases} \tag{7}$$

The temperature adjustment can be done either by a gas-fired boiler or a central air-to-water HP.

2.2. Simulation

The presented component models are now combined to generate the network structure and perform the simulation. The thermal network consists of two subsystems, the warm pipeline system and the cold pipeline system. The representation of the subnetworks is based on the graph theory, where the nodes represent the joints and the edges build the connections between the nodes (pipelines). Within the network, we distinguish between reference nodes, supply nodes, and demand nodes. The reference nodes are located within the EBU to ensure that at least one reference node is included in each subsystem. According to this, the reference nodes set the pressure and temperature values for each system. The supply and demand nodes are located within the substations or the waste heat source, where the values for the mass flow are known and the values for pressure and temperature need to be calculated.

2.2.1. Input data

Input data is required to assign the network parameters for nodes, pipelines, substations, the EBU and the waste heat source(s). The input data is subdivided into two types of inputs given by the user:

- the topology of the network together with the necessary parameters of the pipelines (Fig. 1a)
- the heating and cooling demand of the substations and the supply data of the waste heat source(s), the temperature values of the warm pipeline system, the cold pipeline system and the waste heat source(s) (Fig. 1b)

The input data is stored in several .csv-files for easy accessibility and usage.

The file *nodes.csv* lists all nodes and defines if the node is included as a reference node or a supply/demand node. In case of a reference node the pressure value needs to be specified. The file *pipelines.csv* lists all pipelines of the network and defines inlet and outlet node of each connection. Furthermore, the parameters diameter, length, roughness and thickness of the insulation, heat conductivity of the pipeline material and pipe mode are specified. The pipe mode says if the pipeline is part of the warm or the cold pipeline system. The

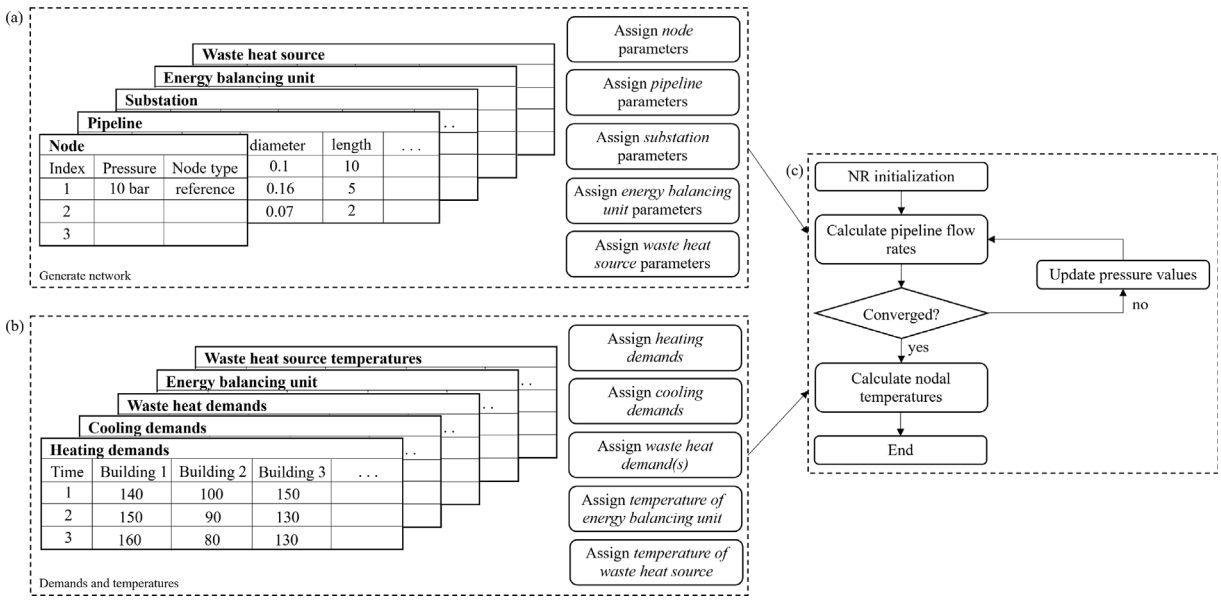

Fig. 1. Usage and solution flow of HeatNetSim.

data for the substations, the EBU and the waste heat sources are stored in the respective files, where inlet and outlet nodes are defined for each component. Further information is necessary for the substations, where the temperature value of the secondary side $T_{set,sec}$ and the temperature differences of the primary and secondary side ΔT_{pri} and ΔT_{sec} are specified. The user can additionally choose between a simple heat exchanger or a HP/compression chiller for exchanging the heat flow with the network. In case one or multiple waste heat sources are to be integrated into the network, the file *wasteHeatSources.csv* contains the temperature difference on the primary side ΔT_{pri}.

The files *heatingDemands.csv*, *coolingDemands.csv* and *wasteHeatDemands.csv* list all components in their columns. If a time series simulation is to be executed, the demand data is given for each time step and stored in the corresponding row. Analogue to the files containing the demand data, the temperature data of the warm and the cold pipeline system is stored in the file *energyBalancingUnitTemperatures.csv*. The temperature values refer to the inlet and outlet node of the EBU. The possibility of varying temperature values is especially relevant when the EBU is not operated on the same temperature over the simulated time scale. In the case of one or several existing waste heat sources, the temperature data of the waste heat is specified analogue to the temperature of the EBU.

Any further parameters not specified by the data tables can be adapted manually within the tool. These parameters could be the ambient temperature, fluid specific parameters (e.g. specific heat capacity, viscosity, density), and parameters concerning the pipe wall material (e.g. specific heat capacity, density).

2.2.2. Solution flow

After setting up the network structure and assigning all necessary parameters, the simulation can be executed. The presented tool uses the Newton–Raphson algorithm (NR) to run the simulation of each time step and solves the problem in an iterative way (Fig. 1c). The process starts with the initialization, where the target flow rate of each node is determined and starting points for unknown nodal pressure and temperature values are set. However, the pressure values of inlet and outlet node of each pipeline cannot be equal, as the mass flow of the pipeline is calculated from the pressure difference between inlet and outlet node. A zero pressure difference leads to a zero flow rate and a poorly conditioned Jacobian matrix. After the initialization, the iterative process starts with the flow rate calculation in each pipeline and the updating of the Jacobian matrix. The value of the actual nodal flow and the target nodal flow is compared and the simulation stops once the error is smaller than the set tolerance. When the simulation is converged, the temperature value of each node is updated and the results are saved.

2.2.3. Time series simulation

Thermal networks are usually not simulated for only one time step, but for multiple time steps. Therefore, HeatNetSim provides the possibility of a time series simulation with varying demand and temperature data. This function is implemented via a loop updating the time depending values in each time step and transferring these to the NR initialization. The simulation process is then executed for each time step individually. For the simulation, the time step length as well as the number of time steps can be specified by the user. Furthermore, HeatNetSim distinguishes between a steady-state simulation and a quasi-dynamic simulation. In case of a quasi-dynamic simulation, time varying values (temperature values) are transmitted between several time steps and taken into account in the following simulation processes.

2.3. Integration into multi energy systems

A coupled investigation of MES becomes more and more relevant within future energy systems. Therefore it is important to analyze the interconnections between multiple energy grids, while at the same time offering detailed grid simulation models for each domain. To achieve this, HeatNetSim enables the calculation of relevant input and output variables for other domains within the coupling components, which can be extracted easily and used for multi domain simulations. The data exchange is also possible between the time steps to take temporally varying interdependencies into account and enable an investigated assessment of different domains. Thus, the coupling to the power sector is for example enabled by the HP model calculating the electricity consumption additionally to the thermal variables. Moreover, as this tool is a further development of the gas network simulation tool GasNetSim, developed by Lu et al. [54,55], the programming structure of both domain's tools is analogue and a coupling between them is straightforward.

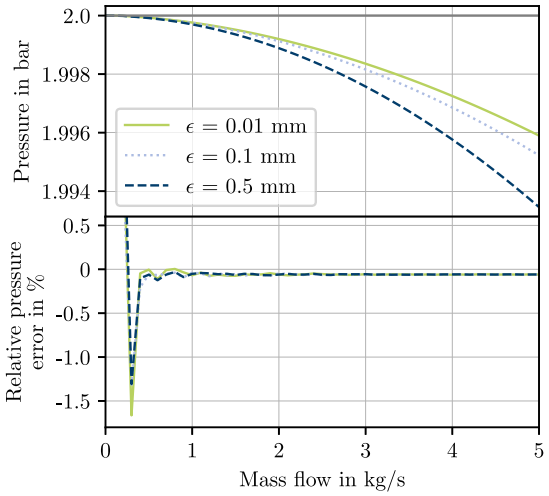

(a) Outlet pressure of one pipeline of the simulation with HeatNetSim (top) and relative error between HeatNetSim and Modelica (bottom).

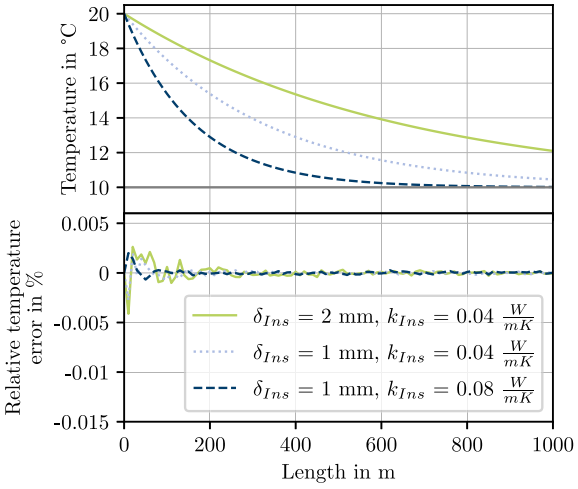

(b) Outlet temperature of one pipeline of the simulation with HeatNetSim (top) and relative error between HeatNetSim and Modelica (bottom).

Fig. 2. Pressure drop and temperature profile: (a) The pressure drop of a pipeline is shown for different mass flow rates considering three values for the roughness ϵ. (b) The temperature profile in a pipeline is shown over the pipeline length for two values of the thickness δ_{Ins} and the heat conductivity k_{Ins} of the insulation. For both pressure and temperature error, the results from HeatNetSim and Modelica are compared.

3. Verification

As this tool has its main focus on the modeling and simulation of thermal networks, the pipeline model is the most important component in order to calculate pressure and temperature values of the network. Due to the lack of standardized test cases for DH networks [56] we use the *PlugFlowPipe*-model [57] as a reference model. The *PlugFlowPipe*-model is a dynamic equation-based thermal-hydraulic pipeline model for DH and DC networks also used in the Modelica-library AixLib [43]. Our verification is carried out for a steady-state simulation with one time step and a quasi-dynamic simulation with multiple time steps. In both cases, the reference model is simulated within the simulation interface Dymola.

3.1. Verification of steady-state simulation

The steady-state verification is performed with the single pipeline model of HeatNetSim and Modelica. Therefore, we keep the inlet pressure and the inlet temperature constant (2 bar and 20 °C). The pressure verification is based on a pipeline with a length of 10 m and a diameter of 0.1 m. We perform three simulation runs with different roughness parameters of the material (0.01 mm, 0.1 mm and 0.5 mm) and vary the mass flow rate between 0 kg/s and 5 kg/s. Fig. 2(a) shows the exponentially decreasing pressure resulting from an increasing mass flow rate. The two models from HeatNetSim and Modelica show very similar results. In order to show the differences of the outlet pressure, the relative error is calculated as the absolute error between the models divided by the pressure drop over the pipeline length in Modelica. For very small mass flow rates, the relative pressure error goes up to 29%, however, the absolute error is not higher than 0.5 Pa for mass flow rates smaller than 0.1 kg/s. For mass flow rates higher than 0.1 kg/s, the relative error lies at around 0.06%.

For the temperature verification, we use a pipeline model with a diameter of 0.1 m and a mass flow rate of 1 kg/s. The values of the thickness and the heat conductivity of the insulation are assumed to 1 mm and 2 mm as well as 0.04 W/(mK) and 0.08 W/(mK), respectively. Fig. 2(b) shows that the temperature approaches the ambient temperature asymptotically, which is set to 10 °C. An increasing pipeline length leads to decreasing heat losses, because of a smaller temperature difference between the fluid and the ambient. By changing the parameters of the insulation, we demonstrate that a smaller thickness and a higher heat conductivity result in higher heat losses over the pipeline length. The comparison between both models shows small temperature differences. The relative error is calculated from the absolute temperature difference between the models divided by the temperature difference over the pipeline length from Modelica. This results in a maximum relative error of 0.004%.

3.2. Verification of the quasi-dynamic simulation

The quasi-dynamic verification is executed with a small network structure consisting of 6 nodes and 4 pipelines, which are connected via an EBU and a substation. Fig. 3 shows the temperature results for the initialization phase simulated with HeatNetSim and Modelica. Both models use the same time step length for their simulation. The system is currently in heating mode, therefore the EBU (node 1) has a constant temperature of 50 °C. The remaining system is initialized with 20 °C in the beginning of the simulation. Each node starts to change its temperature when the fluid arrives at the corresponding node. Due to the thermal inertia of the pipeline wall, the temperature slowly increases up to the target temperature. When the initialization phase is finished, the temperature of node 1, 2, and 3 is according to the warm pipeline system and the temperature of node 4, 5, and 6 is according to the cold pipeline system. Heat losses are not visible within this figure, as the temperature difference between the nodes is not high enough due to the set parameters of the pipelines.

Fig. 3 furthermore shows the influence of the time step length Δt_{step} set in HeatNetSim and Modelica. Fig. 3(a) has a time step length of 1 s resulting in appreciable differences between the models. Decreasing the time step length to 0.01 s (Fig. 3(b)) shows nearly the same results for both models, indicating the mismatch is mainly due to the different numerical methods used.

4. Case studies

In the previous section, we verified the pipeline model for a steady-state and a quasi-dynamic simulation. To test the simulation tool on a realistic network structure and show different use cases, the following section presents two case studies. Case Study 1 refers to a unidirectional DH network with an integrated temperature control of the supply line

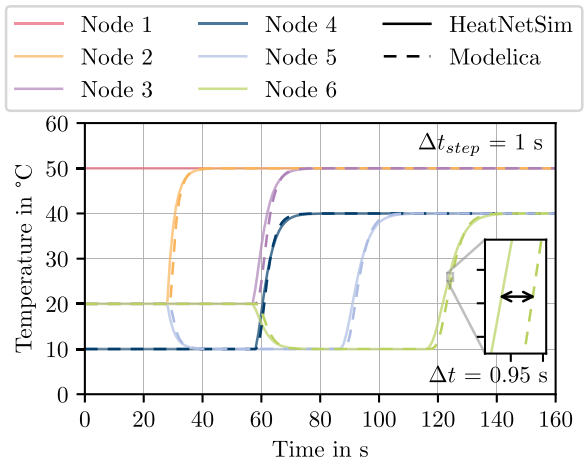

(a) Dynamic temperature calculation with a time step length of 1 s.

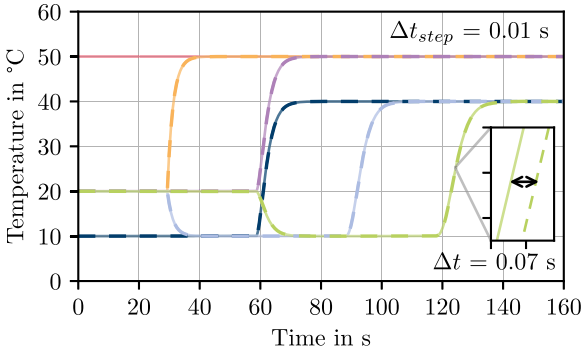

(b) Dynamic temperature calculation with a time step length of 0.01 s.

Fig. 3. Temperature values of a dynamic temperature calculation: The solid lines (simulation with HeatNetSim) and the dashed lines (simulation with Modelica) show the temperature values of the nodes for the initialization phase with heating demands only. Node 1 represents the warm node and node 6 the cold node of the EBU.

and a coupling to the power grid, while Case Study 2 analyzes a bidirectional LTDHC network showing the impact of coupled heating and cooling demands. Both case studies are based on the existing DH network of Forschungszentrum Jülich (FZJ), which is in reality operated on 95 °C to 132 °C. The topology of the DH network consists of 421 nodes and 451 pipelines. 87 buildings are connected to the thermal network, while Case Study 1 additionally uses a CHP plant as a heat source and Case Study 2 a high-performance computer (HPC). For both case studies, one EBU is used to supply the residual heating/cooling demand. The values for the required pipeline parameters diameter, length, roughness, thickness of the insulation, heat transfer coefficient, etc. are according to the actual values of the DH network.

The data for the heating, cooling and electricity demands of each building is based on measured data with a time resolution of 15 min. We use the year 2019 for our analysis. The simulation is run for one week in February to also see the daily fluctuations of the heating and cooling demand.

4.1. Case study 1: A unidirectional DH network

Case Study 1 uses the described network topology to simulate a high temperature DH network with heating demands only. The DH network is coupled to the real power grid of the campus via a CHP plant and integrates the occurring heat into the thermal network. In common applications, the CHP is operated based on the heating demand of the district ensuring a continuous heat supply of all buildings. However, temporally fluctuating electricity demands resulting from PV generation or electric vehicle charging within buildings can in the future be challenging in terms of power supply. Therefore, this case study uses the DH network as a source of flexibility to the power grid by operating the CHP based on the electricity demand. To enable the heat integration at each time step, the supply line temperature of the DH network is adapted according to the occurring amount of heat from the CHP. This case study shows the coupling possibility of HeatNetSim to other domain's simulation tools and furthermore the integration of a variable control algorithm.

4.1.1. Scenario setup

The investigated DH network is in standard mode operated on 80 °C (return line) and 90 °C (supply line). The temperature of the supply line is sufficient to provide the heating energy to the buildings by using a standard heat exchanger.

The operation of the CHP is determined by the electricity demand of the campus $P_{el,CHP}$, simulated with the open-source simulation tool pandapower [40]. The amount of heat $\dot{Q}_{CHP}$ can be calculated from Eq. (8), where η_{th} is the thermal efficiency, set to 0.43, and η_{el} the electrical efficiency, set to 0.34.

$$\dot{Q}_{CHP} = \frac{\eta_{th}}{\eta_{el}} P_{el,CHP} \tag{8}$$

To enable a maximal utilization of the heat from the CHP, the applied temperature control algorithm (Eq. (9)) adapts the supply temperature of the thermal network and consequently uses the thermal inertia of the pipeline system.

$$\Delta T_{adapt} = \frac{\dot{Q}_{CHP} - \dot{Q}_{HD}}{\dot{m}_{flow} c_p} \tag{9}$$

The produced heat temperature of the CHP is assumed to be sufficiently high to be directly integrated into the thermal network via a heat exchanger with an efficiency of 80%.

4.1.2. Results

Fig. 4 shows the electrical and thermal power production of the CHP and the resulting adaptions within the supply line temperature. The power grid simulation of the analyzed campus leads to the required electricity consumption which is exclusively provided by the power-driven CHP. According to Eq. (8), the CHP produces 2405.2 MWh heat over the analyzed time frame of one week. According to the real demand data of our campus, there is a mismatch between the electricity demand and the heating demand. To make sure that the overall waste heat demand of one week is equal to the overall required heating demand, we assume to utilize 85% of the produced CHP-heat and analyze the flexibility potential within this time frame. The heat is consequently used to increase the temperature from the incoming return line to the temperature of the supply line of the DH network. The difference between the produced waste heat and the actual required heat supply in each time step needs to be balanced by the adaption of the supply temperature. According to Fig. 4, the supply temperature is increased from the standard supply temperature when the CHP produces more waste heat than required within the EBU, while the temperature is decreased when the occurring waste heat is not sufficient to balance the heating demand of the network. This leads to fluctuations within the supply line temperature from 80.7 °C to 110.0 °C. In case of an actually planned transformation towards a power-driven CHP operation, temperature requirements of the supplied buildings need to be checked and back-up mechanisms such as gas boilers are necessary.

The results of the applied thermal-hydraulic network simulation of the DH network are shown in Fig. 5. Hereby, the thickness of the lines represents the mass flow value of each pipeline and the arrows indicate the direction of the flow at this specific time step. According to the

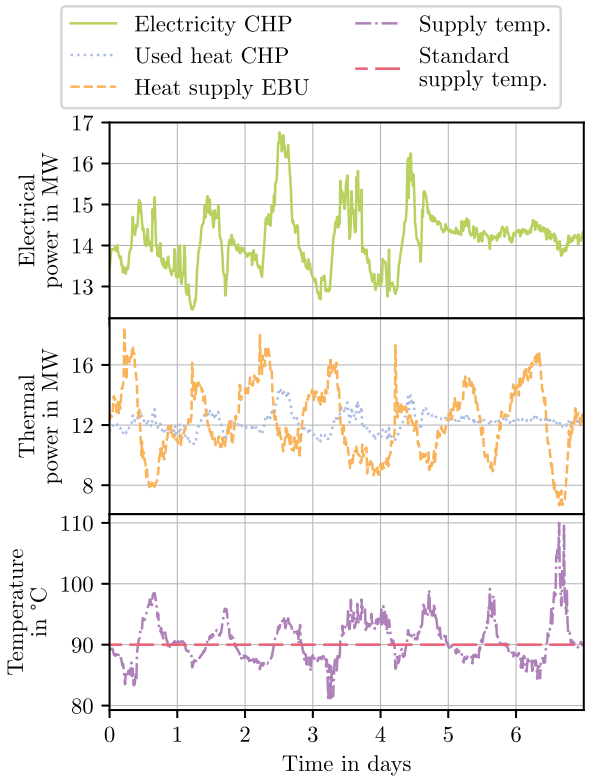

Fig. 4. Electrical and thermal power over one week: The grid-connected buildings of FZJ lead to the electricity consumption, simulated with the open-source simulation tool pandapower. The electricity-driven CHP produces the heat according to the applied CHP-model, while the actual heating demand is generated with HeatNetSim.

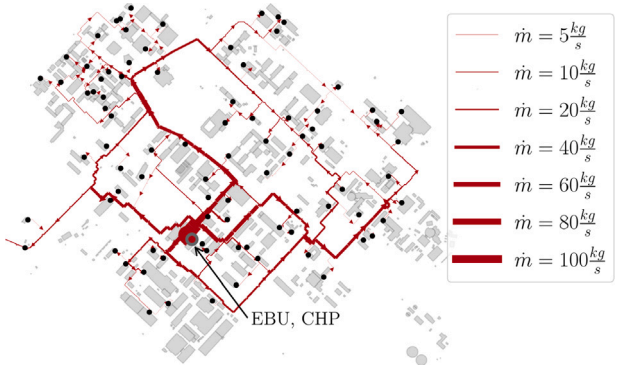

Fig. 5. Network topology of the unidirectional DH network: The thickness of the lines represents the value of the mass flow rate in each pipeline and the arrow indicates the direction of the flow. The black dots refer to the buildings and the red/gray dot to the EBU and the CHP.

functioning of an unidirectional thermal network, the heat is supplied centrally and distributed according to the decentral requirements to the substations. This leads to a maximum mass flow at the EBU and to decreasing flow rates towards the grid-connected buildings.

4.2. Case study 2: A bidirectional LTDHC network

With an increasing electrification of the heating sector via HPs and additionally a rising demand for cooling energy, lower network operating temperatures become more and more reasonable. This enables a simultaneous supply of heating and cooling energy and, thus, can lead to energy efficient thermal balancing effects. To investigate the occurring potential, this case study transforms the originally separately managed DH and DC network of FZJ into a bidirectional LTDHC network and integrates the waste heat from the existing HPC. We simulate the network structure with HeatNetSim and analyze the energy saving potential of the coupling together with the occurring impacts on the grid infrastructure.

4.2.1. Scenario setup

The analyzed LTDHC network is operated on 20 °C (cold pipeline system) and 30 °C (warm pipeline system). However, the required demand temperature on the building side is higher than the warm network temperature and HPs with a temperature difference of 10 K on the secondary side are assumed within the buildings. To investigate the influence of the HP operation on the network, we choose three different demand temperatures: 40 °C, 60 °C and 80 °C. This shows the effects of the demand temperature on the overall electricity consumption and the behavior of the network. The temperature gap between the network and the demand also occurs for the cooling energy, resulting in additional compression chillers in the buildings with cooling demands.

The waste heat provided by the HPC has a temperature of 30 °C to 40 °C. Therefore, we assume that a heat exchanger with an efficiency of 80% is sufficient to integrate the waste heat into the LTDHC network.

4.2.2. Results

Fig. 6 shows the heating and cooling demand of the grid-connected buildings, together with the waste heat from the HPC over the analyzed time frame. The simulation results show that, in all three scenarios, the heating and cooling energy can balance each other to a certain extent. The residual demand is then covered by the EBU, while a positive value means an additional heat supply and a negative value an additional cooling supply. The shown electrical power is consumed by the HPs and compression chillers in the buildings in order to increase or decrease the temperature of the fluid to meet the demand temperature. Hereby, the electrical power consumed by the circulation pumps is not part of the analysis, as the focus lies on the energy saving potential coming from thermal balancing effects. Within the three analyzed scenarios, a higher temperature difference between the evaporator and the condensator side of the HP results in a reduced COP and a higher electrical power consumption. Hereby, using a demand temperature of 40 °C and 60 °C leads to similar simulation results. This can be explained by the defined upper limit of the COP, which is set to 6 within this case study in order to prevent unrealistic efficiencies of the HP.

The different values of the COP result in a slightly changed energy efficiency and a change in the location of the energy consumption (Fig. 8). While the lowest demand temperature has an overall energy consumption of 926.9 MWh, a high share of the energy is provided within the EBU, indicated as heating supply in the figure. The highest demand temperature consumes 951.5 MWh energy, which is mostly supplied via electrical energy within the substations. In all three scenarios, clear thermal balancing effects can be achieved by the bidirectionality of the network, as the overall heating and cooling demand lies at 1820.7 MWh and 1069.8 MWh, respectively. This stresses an improvement by coupling heating and cooling demands in a campus with variable thermal requirements.

However, transforming an unidirectional DH network into a bidirectional DHC network can have impacts on network internal variables, which can be revealed by the applied thermal-hydraulic simulation (Fig. 7(a)). The previously mentioned balancing effects are clearly visible as the pipelines connected to the EBU transport only comparably small mass flows. In contrast, the mass flow nearby the HPC whose waste heat is constantly fed into the network is significantly larger.

This requires a more detailed look into the pipeline diameters, as excessive pressure drops may occur in some parts of the network. Fig. 7(b) therefore shows the diameter values of the network indicated by the thickness of the lines. We calculate the pressure drop per unit length for each pipeline by using the maximal occurring mass flow rate in the corresponding pipeline segment. The pressure drop per unit

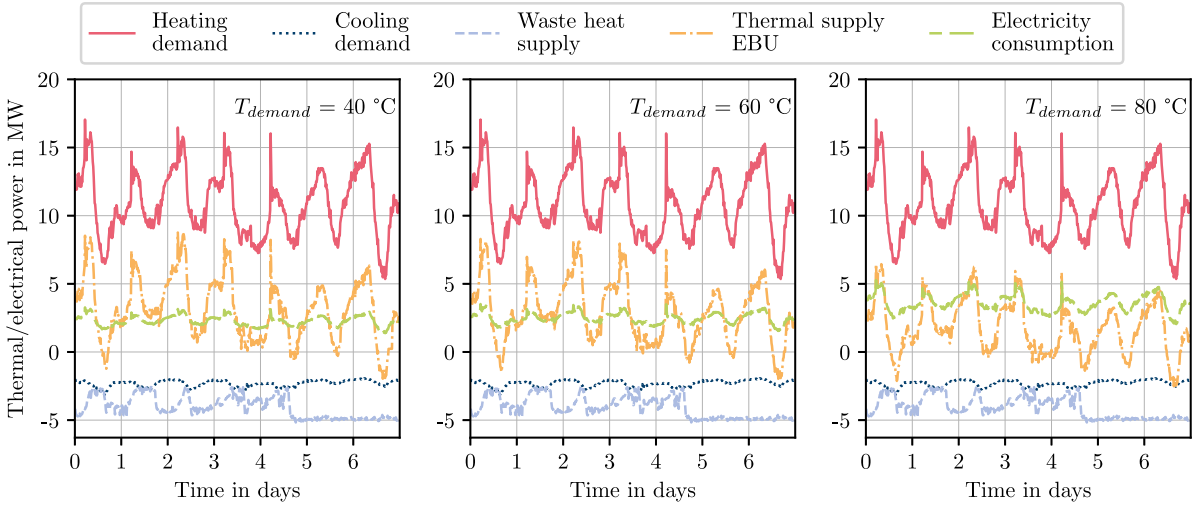

Fig. 6. Thermal and electrical power over one week: The time series of the heating and cooling demand and the waste heat supply lead to the thermal supply of the EBU and the electrical power consumption of the HPs and compression chillers. The thermal and electrical power is shown for the three demand temperature levels 40 °C (left), 60 °C (middle) and 80 °C (right).

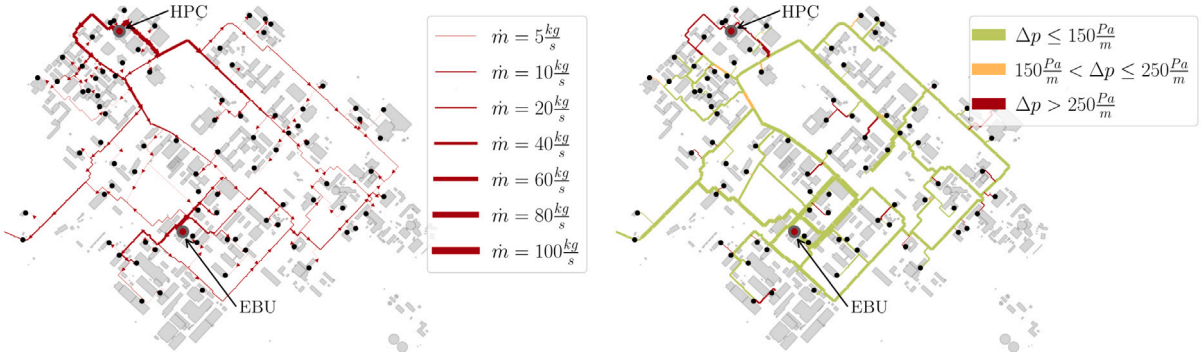

(a) Mass flow within bidirectional network with heating and cooling demands and HPC.

(b) Diameter values within bidirectional network together with pressure drops of pipelines.

Fig. 7. Network topology of the bidirectional LTDHC network: In Figure (a), the thickness of the lines represents the value of the mass flow rate in each pipeline and the arrow indicates the direction of the flow. In Figure (b), the thickness of the lines represents the diameter of the pipeline and the color indicates the pressure drop per unit length. The results are generated for a demand temperature of 60 °C. The black dots refer to the buildings and the red/gray dot to the EBU and the HPC.

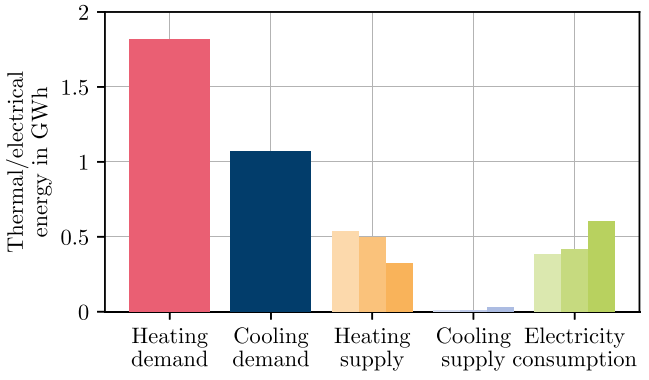

Fig. 8. Thermal and electrical energy for one week: The heating and cooling demand over one week lead to the heating and cooling supply of the EBU and the electrical power consumption of the HPs and compression chillers. The cooling demand includes the waste heat. The thermal and electrical power consumption is clustered into the three demand temperature levels 40 °C (left), 60 °C (middle) and 80 °C (right).

length should not exceed 200 Pa/m to 250 Pa/m [53,58,59] to limit the power consumption of the circulation pumps. Consequently, the hydraulic pipeline simulation demonstrates that certain parts of the network structure might be undersized when transforming a unidirectional thermal network into a bidirectional one, especially when integrating an additional waste heat source.

5. Conclusion

The usage of thermal networks can accelerate the decarbonization targets of the heating and cooling sector to supply buildings. Advanced concepts for the operation of DH networks, coupling to other energy sectors and the integration of waste heat sources requires suitable thermal-hydraulic modeling and simulation tools. In order to analyze the potential of bidirectional DHC networks, these tools must furthermore enable flow reversion and a zero mass flow rate. This work presents an open-source simulation tool for uni- and bidirectional networks, which is capable of the mentioned properties. The modeling of the required components is explained and the simulation flow based on the generated network structure is presented. The results of the steady-state and quasi-dynamic simulation of the pipeline model are verified with the *PlugFlowPipe*-model developed by Van der Heijde et al. [57].

With the two presented case studies we demonstrate the functionalities of the developed simulation tool for unidirectional and bidirectional thermal networks. The basis of both case studies is the existing DH network of the FZJ-campus, which has 421 nodes and 451 pipelines. Case Study 1 refers to a high temperature DH network which is coupled to the power sector via a CHP plant. The power sector is represented by the real power grid of the FZJ-campus, simulated with the open-source simulation tool pandapower. According to the operation of the CHP, which is based on the electricity demand of the campus, the DH network provides flexibility to the power grid. We show that by an appropriate adaption of the supply temperature, the DH network can be exclusively supplied by the heat from the CHP. The supply temperature therefore fluctuates between 80.7 °C and 110.0 °C, while the standard supply temperature lies at 90 °C. However, as expected for coupled power and heating networks, there is a mismatch between the overall electricity and heating demand over the analyzed time frame. To overcome this mismatch and enable a maximal utilization of the occurring CHP-heat, additional thermal or electrical storages or import/export options to neighboring districts could be beneficial. Moreover, a broader time frame and consequently larger temperature adaptions of the supply temperature might increase the amount of waste heat integration. However, the building's heating supply with sufficiently high temperatures need to be ensured what can be checked by a thermal-hydraulic network simulation.

Case Study 2 transforms the DH and DC network of FZJ into a bidirectional LTDHC network and integrates the existing HPC as a waste heat source. The thermal-hydraulic network simulation shows that grid-internal balancing effects lead to an energy consumption of 926.9 MWh for a demand temperature of 40 °C and to 951.5 MWh for a demand temperature of 80 °C, while having an overall heating and cooling demand of 2890.5 MWh. However, we show that the transformation from an unidirectional to a bidirectional network is linked to obstacles concerning the pressure drop within the pipelines. Pipeline diameters are designed for the operation of the unidirectional system which might lead to bottlenecks. In our case study bottlenecks mainly occur in the area of the waste heat source. However, large parts of the network infrastructure are oversized due to generally higher mass flow values within a network designed for a unidirectional supply. This aspect is left out within the performed analyzes, as minimal pressure drop values are hard to define in a network with changing flow directions.

Availability of HeatNetSim

https://jugit.fz-juelich.de/iek-10/public/simulation/heatnetsim

CRediT authorship contribution statement

Sina Dibos: Writing – review & editing, Writing – original draft, Visualization, Validation, Software, Resources, Methodology, Investigation, Formal analysis, Data curation, Conceptualization. **Thiemo Pesch:** Writing – review & editing, Supervision, Project administration, Funding acquisition, Conceptualization. **Andrea Benigni:** Writing – review & editing, Supervision, Project administration, Funding acquisition, Conceptualization.

Declaration of competing interest

The authors declare that they have no known competing financial interests or personal relationships that could have appeared to influence the work reported in this paper.

Appendix A. Hydraulic calculation of pipeline model

The Reynolds number $Re_{laminar}$ is used to distinguish between laminar and turbulent flows. In case of a laminar flow, the friction factor f can be expressed according to Eq. (A.1) [60]:

$$f = \frac{64}{Re_{laminar}}. \tag{A.1}$$

The Reynolds number depends on the diameter D of the pipeline, the density ρ, the mean velocity $\bar{v}$ and the viscosity μ of the fluid:

$$Re_{laminar} = \frac{\rho \bar{v} D}{\mu}. \tag{A.2}$$

The pressure difference between the inlet and outlet node Δp can be expressed according to Eq. (A.3) with l being the length of the pipeline.

$$\Delta p = f \frac{l}{D} \frac{\rho}{2} \bar{u}^2 \tag{A.3}$$

The mass flow rate is consequently calculated according to Eq. (A.4).

$$\dot{m}_{laminar} = \frac{1}{128} \Delta p \pi \frac{D^4 \rho}{l \mu} \tag{A.4}$$

In case of a turbulent flow, the Prandtl–Colebrook equation for turbulent flows is applied [60] where k_s is the roughness of the material:

$$\frac{1}{\sqrt{f}} = -2log\left(\frac{k_s/D}{3.71} + \frac{2.51}{Re_{turbulent}\sqrt{f}}\right). \tag{A.5}$$

The mass flow rate for a turbulent flow can then be determined by using the Reynolds number $Re_{turbulent}$ from Eq. (A.6).

$$\dot{m}_{turbulent} = \frac{A}{D} \mu Re_{turbulent} \tag{A.6}$$

Appendix B. Heat loss calculation of pipeline model

Eq. (B.1) represents the differential equation for the temperature calculation of one pipeline segment. Here, $\dot{m}$ is the mass flow rate, c_p is the specific heat capacity, T the fluid temperature, l the pipeline length, α the heat transfer coefficient and T_{amb} the ambient temperature [60].

$$\dot{m} c_p \frac{dT}{dl} = \alpha (T_{amb} - T) \tag{B.1}$$

Solving the differential equation leads to Eq. (B.2):

$$T(l) = (T(t_{in}, l_0) - T_{amb}) \cdot exp\left(-\frac{\alpha l}{\dot{m} c_p}\right) + T_{amb}. \tag{B.2}$$

The heat transfer coefficient α is written as $\alpha = 1/R$. The thermal resistance per unit length R is calculated from Eq. (B.3), where λ is the heat conductivity of the pipeline material, r_1 the radius of the pipeline with insulation and r_2 the radius without insulation.

$$R = \frac{log\left(\frac{r_2}{r_1}\right)}{2\pi\lambda} \tag{B.3}$$

The calculated outlet temperature of each pipeline is then stored in the outlet node of the pipeline. In case a node is supplied by two or more pipelines (to represent a junction within the thermal network), the node temperature is calculated as a mixture of the incoming flows, considering their specific mass flow rates:

$$T_{node} = \frac{T_{in,1}\dot{m}_{in,1} + \cdots + T_{in,n}\dot{m}_{in,n}}{\sum_{i=1}^{n} \dot{m}_{in,i}} \tag{B.4}$$

Appendix C. Heat exchanger

$\dot{Q}_{HD}$ represents the heating demand and $\dot{Q}_{CD}$ the cooling demand of the building. $\dot{Q}_{network}$ is the heat flow transmitted to the network or extracted from the network and η_{HE} the efficiency of the heat exchanger:

$$\begin{aligned} \dot{Q}_{HD} &= \eta_{HE} \dot{Q}_{network}, \\ \eta_{HE} \dot{Q}_{CD} &= \dot{Q}_{network}. \end{aligned} \tag{C.1}$$

Appendix D. Heat pump

Eq. (D.1) specifies the relation between the heating demand, the thermal power extracted from the network and the electrical power $P_{el,HP}$ of the HP.

$$\dot{Q}_{HD} = \dot{Q}_{network} + P_{el,HP} \tag{D.1}$$

The electrical power can be substituted by Eq. (D.2):

$$P_{el,HP} = \frac{\dot{Q}_{HD}}{COP_{HP}}. \tag{D.2}$$

The coefficient of performance COP_{HP} of the HP depends on the demand temperature of the building T_{demand} and the network temperature $T_{network,in}$ [53]. The efficiency factor η is set to 0.5 within this model:

$$COP_{HP} = \eta \frac{T_{demand}}{T_{demand} - T_{network,in}}. \tag{D.3}$$

Appendix E. Compression chiller

The thermal power on the primary side of the compression chiller is calculated from the cooling demand of the building $\dot{Q}_{CD}$ and the electrical power consumption of the compression chiller $P_{el,chiller}$ (Eq. (E.1)). Within this model, we set the efficiency of the compression chiller to 5.

$$\dot{Q}_{CD} + P_{el,chiller} = \dot{Q}_{network} \tag{E.1}$$

Data availability

The authors do not have permission to share data.

References

[1] European Commission. Heating and cooling. 2023, URL https://energy.ec.europa.eu/topics/energy-efficiency/heating-and-cooling_en.

[2] International Energy Agency. Heating. 2023, URL https://www.iea.org/energy-system/buildings/heating.

[3] European Environment Agency. Decarbonisation heating and cooling - A climate imperative. 2023, URL https://www.eea.europa.eu/publications/decarbonisation-heating-and-cooling.

[4] Hiltunen P, Syri S. Low-temperature waste heat enabling abandoning coal in espoo district heating system. Energy 2021;231:120916. http://dx.doi.org/10.1016/j.energy.2021.120916.

[5] Mazhar AR, Liu S, Shukla A. A state of art review on the district heating systems. Renew Sustain Energy Rev 2018;96:420–39. http://dx.doi.org/10.1016/j.rser.2018.08.005.

[6] Malcher X, Gonzalez-Salazar M. Strategies for decarbonizing European district heating: Evaluation of their effectiveness in Sweden, France, Germany, and Poland. Energy 2024;306:132457. http://dx.doi.org/10.1016/j.energy.2024.132457.

[7] Edtmayer H, Nageler P, Heimrath R, Mach T, Hochenauer C. Investigation on sector coupling potentials of a 5th generation district heating and cooling network. Energy 2021;230:120836. http://dx.doi.org/10.1016/j.energy.2021.120836.

[8] Wang W, Jing S, Sun Y, Liu J, Niu Y, Zeng D, et al. Combined heat and power control considering thermal inertia of district heating network for flexible electric power regulation. Energy 2019;169:988–99. http://dx.doi.org/10.1016/j.energy.2018.12.085.

[9] Lund H, Werner S, Wiltshire R, Svendsen S, Thorsen JE, Hvelplund F, et al. 4Th generation district heating (4GDH). Energy 2014;68:1–11. http://dx.doi.org/10.1016/j.energy.2014.02.089.

[10] European Commission. Fifth generation, low temperature, high exergy district heating and cooling networks. 2015, URL https://cordis.europa.eu/project/id/649820/factsheet.

[11] Lund H, Østergaard PA, Nielsen TB, Werner S, Thorsen JE, Gudmundsson O, et al. Perspectives on fourth and fifth generation district heating. Energy 2021;227:120520. http://dx.doi.org/10.1016/j.energy.2021.120520.

[12] Lund H, Østergaard PA, Chang M, Werner S, Svendsen S, Sorknæs P, et al. The status of 4th generation district heating: Research and results. Energy 2018;164:147–59. http://dx.doi.org/10.1016/j.energy.2018.08.206.

[13] Meibodi SS, Loveridge F. The future role of energy geostructures in fifth generation district heating and cooling networks. Energy 2022;240:122481. http://dx.doi.org/10.1016/j.energy.2021.122481.

[14] Gjoka K, Rismanchi B, Crawford RH. Fifth-generation district heating and cooling: Opportunities and implementation challenges in a mild climate. Energy 2024;286:129525. http://dx.doi.org/10.1016/j.energy.2023.129525.

[15] Munćan V, Mujan I, Macura D, Anđelković AS. The state of district heating and cooling in Europe - A literature-based assessment. Energy 2024;304:132191. http://dx.doi.org/10.1016/j.energy.2024.132191.

[16] Østergaard DS, Smith KM, Tunzi M, Svendsen S. Low-temperature operation of heating systems to enable 4th generation district heating: A review. Energy 2022;248:123529. http://dx.doi.org/10.1016/j.energy.2022.123529.

[17] Cross H. Analysis of flow in networks of conduits or conductors. 1936.

[18] Liu X, Wu J, Jenkins N, Bagdanavicius A. Combined analysis of electricity and heat networks. Appl Energy 2016;162:1238–50. http://dx.doi.org/10.1016/j.apenergy.2015.01.102.

[19] Dancker J, Wolter M. Improved quasi-steady-state power flow calculation for district heating systems: A coupled Newton-Raphson approach. Appl Energy 2021;295:116930. http://dx.doi.org/10.1016/j.apenergy.2021.116930.

[20] Rüdiger J. Enhancements of the numerical simulation algorithm for natural gas networks based on node potential analysis. IFAC-PapersOnLine 2020;53(2):13119–24. http://dx.doi.org/10.1016/j.ifacol.2020.12.2282.

[21] Wang Y, Wang X, Zheng L, Gao X, Wang Z, You S, et al. Thermo-hydraulic coupled analysis of long-distance district heating systems based on a fully-dynamic model. Appl Therm Eng 2023;222:119912. http://dx.doi.org/10.1016/j.applthermaleng.2022.119912.

[22] Zhang S, Gu W, Lu S, Yao S, Zhou S, Chen X. Dynamic security control in heat and electricity integrated energy system with an equivalent heating network model. IEEE Trans Smart Grid 2021;12(6):4788–98. http://dx.doi.org/10.1109/TSG.2021.3102057.

[23] Steinegger J, Wallner S, Greiml M, Kienberger T. A new quasi-dynamic load flow calculation for district heating networks. Energy 2023;266:126410. http://dx.doi.org/10.1016/j.energy.2022.126410.

[24] Leitner B, Widl E, Gawlik W, Hofmann R. A method for technical assessment of power-to-heat use cases to couple local district heating and electrical distribution grids. Energy 2019;182:729–38. http://dx.doi.org/10.1016/j.energy.2019.06.016.

[25] Dancker J, Wolter M. A joined quasi-steady-state power flow calculation for integrated energy systems. IEEE Access 2022;10:33586–601. http://dx.doi.org/10.1109/ACCESS.2022.3161961.

[26] Oppelt T, Urbaneck T, Gross U, Platzer B. Dynamic thermo-hydraulic model of district cooling networks. Appl Therm Eng 2016;102:336–45. http://dx.doi.org/10.1016/j.applthermaleng.2016.03.168.

[27] Dénarié A, Aprile M, Motta M. Heat transmission over long pipes: New model for fast and accurate district heating simulations. Energy 2019;166:267–76. http://dx.doi.org/10.1016/j.energy.2018.09.186.

[28] Dénarié A, Aprile M, Motta M. Dynamical modelling and experimental validation of a fast and accurate district heating thermo-hydraulic modular simulation tool. Energy 2023;282:128397. http://dx.doi.org/10.1016/j.energy.2023.128397.

[29] Qin X, Sun H, Shen X, Guo Y, Guo Q, Xia T. A generalized quasi-dynamic model for electric-heat coupling integrated energy system with distributed energy resources. Appl Energy 2019;251:113270. http://dx.doi.org/10.1016/j.apenergy.2019.05.073.

[30] Benonysson A. Dynamic modelling and operational optimization of district heating systems. 1991.

[31] Ben Hassine I, Eicker U. Impact of load structure variation and solar thermal energy integration on an existing district heating network. Appl Therm Eng 2013;50(2):1437–46. http://dx.doi.org/10.1016/j.applthermaleng.2011.12.037.

[32] Stevanovic VD, Zivkovic B, Prica S, Maslovaric B, Karamarkovic V, Trkulja V. Prediction of thermal transients in district heating systems. Energy Convers Manage 2009;50(9):2167–73. http://dx.doi.org/10.1016/j.enconman.2009.04.034.

[33] Wang H, Wang H, Zhu T. A new hydraulic regulation method on district heating system with distributed variable-speed pumps. Energy Convers Manage 2017;147:174–89. http://dx.doi.org/10.1016/j.enconman.2017.03.059.

[34] STANET. STANET - Network analysis for gas, water, electricity, district heating and sewage, URL https://www.stafu.de/en/product.html.

[35] TRNSYS: Transsolar softwareengineering, URL https://trnsys.de/.

[36] RZVN Wehr GmbH. ROKA3, URL https://roka3.com/.

[37] Pfenninger S, Hirth L, Schlecht I, Schmid E, Wiese F, Brown T, et al. Opening the black box of energy modelling: Strategies and lessons learned. Energy Strategy Rev 2018;19:63–71. http://dx.doi.org/10.1016/j.esr.2017.12.002.

[38] Röder J, Meyer B, Krien U, Zimmermann J, Stührmann T, Zondervan E. Optimal design of district heating networks with distributed thermal energy storages – method and case study. Int J Sustain Energy Plan Manag 2021;31:5–22. http://dx.doi.org/10.5278/IJSEPM.6248, 2021.

[39] Vorspel L, Bücker J. District-heating-grid simulation in python: Digripy. Computation 2021;9(6):72. http://dx.doi.org/10.3390/computation9060072.

[40] Lohmeier D, Cronbach D, Drauz SR, Braun M, Kneiske TM. Pandapipes: An open-source piping grid calculation package for multi-energy grid simulations. Sustainability 2020;12(23):9899. http://dx.doi.org/10.3390/su12239899.

[41] nPro - Planning tool for buildings and districts, URL https://www.npro.energy/main/de/.

[42] Technische Universität Hamburg. TransiEnt library, URL https://www.tuhh.de/transient-ee/.
[43] Maier L, Jansen D, Wüllhorst F, Kremer M, Kümpel A, Blacha T, et al. AixLib: an open-source modelica library for compound building energy systems from component to district level with automated quality management. J Build Perform Simul 2023. http://dx.doi.org/10.1080/19401493.2023.2250521.
[44] Jorissen F, Reynders G, Baetens R, Picard D, Saelens D. Implementation and verification of the IDEAS building energy simulation library. J Build Perform Simul 2018.
[45] García-Céspedes J, Herms I, Arnó G, de Felipe JJ. Fifth-generation district heating and cooling networks based on shallow geothermal energy: A review and possible solutions for Mediterranean Europe. 2023, http://dx.doi.org/10.3390/en16010147.
[46] Thurner L, Scheidler A, Schafer F, Menke J-H, Dollichon J, Meier F, et al. Pandapower—An open-source python tool for convenient modeling, analysis, and optimization of electric power systems. IEEE Trans Power Syst 2018;33(6):6510–21. http://dx.doi.org/10.1109/TPWRS.2018.2829021.
[47] Brunnemann J, Gottelt F, Wellner K, Renz A, Thüring A, Roeder V, et al. Status of ClaRaCCS: Modelling and simulation of coal-fired power plants with CO2 capture. In: Proceedings of the 9th international MODELICA conference, September 3-5, 2012, munich, Germany. Linköping electronic conference proceedings, Linköping University Electronic Press; 2012, p. 609–18. http://dx.doi.org/10.3384/ecp12076609.
[48] Andresen L, Dubucq P, Garcia RP, Ackermann G, Kather A, Schmitz G. Status of the TransiEnt library: Transient simulation of coupled energy networks with high share of renewable energy. 2015.
[49] Senkel A, Schmitz G. Using modelica to assess the resilience of a heat supply system. In: Corrado V, Fabrizio E, Gasparella A, Patuzzi F, editors. Proceedings of building simulation 2019: 16th conference of IBPSA. Building simulation conference proceedings, IBPSA; 2020, p. 1941–7. http://dx.doi.org/10.26868/25222708.2019.210780.
[50] Müller D, Lauster M, Constantin A, Fuchs M, Remmen P. AIXLIB - An open-source modelica library within the IEA-EBC ANNEX 60 framework. In: BauSIM 2016. 2016.
[51] Schweiger G, Heimrath R, Falay B, O'Donovan K, Nageler P, Pertschy R, et al. District energy systems: Modelling paradigms and general-purpose tools. Energy 2018;164:1326–40. http://dx.doi.org/10.1016/j.energy.2018.08.193.
[52] Guelpa E. Impact of network modelling in the analysis of district heating systems. Energy 2020;213:118393. http://dx.doi.org/10.1016/j.energy.2020.118393.
[53] Sommer T, Sulzer M, Wetter M, Sotnikov A, Mennel S, Stettler C. The reservoir network: A new network topology for district heating and cooling. Energy 2020;199:117418. http://dx.doi.org/10.1016/j.energy.2020.117418.
[54] Lu Y, Pesch T, Benigni A. Simulation of coupled power and gas systems with hydrogen-enriched natural gas. Energies 2021;14(22):7680. http://dx.doi.org/10.3390/en14227680.
[55] Lu Y, Pesch T, Benigni A. GasNetSim: An open-source package for gas network simulation with complex gas mixture compositions. In: 2022 open source modelling and simulation of energy systems. IEEE; 2022, p. 1–6. http://dx.doi.org/10.1109/OSMSES54027.2022.9769148.
[56] Kuntuarova S, Licklederer T, Huynh T, Zinsmeister D, Hamacher T, Perić V. Design and simulation of district heating networks: A review of modeling approaches and tools. Energy 2024;132189. http://dx.doi.org/10.1016/j.energy.2024.132189.
[57] van der Heijde B, Fuchs M, Ribas Tugores C, Schweiger G, Sartor K, Basciotti D, et al. Dynamic equation-based thermo-hydraulic pipe model for district heating and cooling systems. Energy Convers Manage 2017;151:158–69. http://dx.doi.org/10.1016/j.enconman.2017.08.072.
[58] Gudmundsson O, Schmidt R-R, Dyrelund A, Thorsen JE. Economic comparison of 4GDH and 5GDH systems – using a case study. Energy 2022;238:121613. http://dx.doi.org/10.1016/j.energy.2021.121613.
[59] Nussbaumer T, Thalmann S. Influence of system design on heat distribution costs in district heating. Energy 2016;101:496–505. http://dx.doi.org/10.1016/j.energy.2016.02.062.
[60] Velut S, Tummescheit H. Implementation of a transmission line model for fast simulation of fluid flow dynamics. In: Proceedings 8th modelica conference, Dresden, Germany, March 20-22, 2011. 2011.